

ORIGINAL ARTICLE

NF1 germline mutation differentially dictates optic glioma formation and growth in neurofibromatosis-1

Joseph A. Toonen¹, Corina Anastasaki¹, Laura J. Smithson¹, Scott M. Gianino¹, Kairong Li², Robert A. Kesterson² and David H. Gutmann^{1,*}¹Department of Neurology, Washington University School of Medicine, PO Box 8111, 660 S. Euclid Avenue, St. Louis, MO 63110, USA and ²Department of Genetics, University of Alabama, Birmingham, AL 35233, USA

*To whom correspondence should be addressed. Tel: +314 362 7379; Fax: +314 362 2388; Email: gutmann@neuro.wustl.edu

Abstract

Neurofibromatosis type 1 (NF1) is a common neurogenetic condition characterized by significant clinical heterogeneity. A major barrier to developing precision medicine approaches for NF1 is an incomplete understanding of the factors that underlie its inherent variability. To determine the impact of the germline *NF1* gene mutation on the optic gliomas frequently encountered in children with NF1, we developed genetically engineered mice harboring two representative NF1-patient-derived *Nf1* gene mutations (c.2542G>C;p.G848R and c.2041C>T;p.R681X). We found that each germline *Nf1* gene mutation resulted in different levels of neurofibromin expression. Importantly, only R681X^{CKO} but not G848R^{CKO} mice develop optic gliomas with increased optic nerve volumes, glial fibrillary acid protein immunoreactivity, proliferation and retinal ganglion cell death, similar to *Nf1* conditional knockout mice harboring a neomycin insertion (neo) as the germline *Nf1* gene mutation. These differences in optic glioma phenotypes reflect both cell-autonomous and stromal effects of the germline *Nf1* gene mutation. In this regard, primary astrocytes harboring the R681X germline *Nf1* gene mutation exhibit increased basal astrocyte proliferation (BrdU incorporation) indistinguishable from neo^{CKO} astrocytes, whereas astrocytes with the G848R mutation have lower levels of proliferation. Evidence for paracrine effects from the tumor microenvironment were revealed when R681X^{CKO} mice were compared with conventional neo^{CKO} mice. Relative to neo^{CKO} mice, the optic gliomas from R681X^{CKO} mice had more microglia infiltration and JNK^{Thr183/Tyr185} activation, microglia-produced Ccl5, and glial AKT^{Thr308} activation. Collectively, these studies establish that the germline *Nf1* gene mutation is a major determinant of optic glioma development and growth through by both tumor cell-intrinsic and stromal effects.

Introduction

Neurofibromatosis type 1 (NF1) is a common genetic disorder, affecting 1 in 3000 people worldwide (1). While NF1 is a classic autosomal dominant inherited monogenic condition with complete penetrance, expression of the clinical features of this disorder is extremely variable (2,3). In this regard, children and adults with NF1 are at risk for developing a wide range of medical problems, including benign and malignant peripheral nerve sheath tumors, bone defects, cognitive and attentional deficits, heart defects, breast cancer, autism and brain tumors. Unfortunately, it is currently not possible to predict which of these

various clinical abnormalities will manifest in any given individual. The lack of prognostic risk factors to guide patient management represents one of the most significant barriers to actualizing personalized (precision) medicine strategies for children and adults affected with NF1.

Converging evidence from epidemiologic and human NF1-patient-induced pluripotent stem cell (iPSC) studies has raised the possibility that the germline NF1 gene mutation may be one such predictive risk factor. As such, several groups have reported genotype–phenotype correlations, including clustering of 5′-tertile NF1 gene mutations in individuals with NF1 optic pathway glioma (OPG) (4,5) and two specific germline NF1 gene mutations

Received: September 14, 2015. Revised: December 16, 2015. Accepted: February 8, 2016

© The Author 2016. Published by Oxford University Press. All rights reserved. For Permissions, please email: journals.permissions@oup.com

in people who do not develop cutaneous neurofibromas [c.2970-2972_{del}AAT; (6); c.5425C>T; (7)]. In addition, patients with large 1.4 Mb genomic microdeletions, including the entire NF1 gene locus, have an increased number of neurofibromas and are at an elevated risk for cardiac malfunction, skeletal anomalies, facial dysmorphism, and malignant tumor development (8). Moreover, studies employing NF1-patient-derived iPSCs and derivative neural progenitor (NP) cells have recently revealed that different NF1 germline mutations have distinct effects on NF1 protein (neurofibromin) expression and function (9). While these early-phase genotype–phenotype studies are intriguing, the potential mechanistic impact of the germline NF1 gene mutation on disease pathogenesis has not been formally investigated.

One of the most common tumors affecting children with NF1 is the OPG (10). In this regard, 15–20% of children with NF1 develop World Health Organization grade I pilocytic astrocytomas, a low-grade brain tumor characterized by low proliferative indices and infiltration of microglia (11). While seldom fatal, these OPGs are often associated with visual decline (12,13). Over the past two decades, the cellular and molecular mechanisms responsible for NF1-associated optic glioma (14,15) have been investigated using genetically engineered mouse (GEM) models, resulting in the identification of several promising therapeutic drug targets (16,17). However, these *Nf1* mutant mice harbor a germline inactivating disruption of the murine *Nf1* gene created by introducing a neomycin targeting cassette into exon 31, a mutation not found in people with NF1 (18,19). In this regard, the impact of this knockout allele could either under- or over-represent the effects of actual NF1-patient germline *Nf1* gene mutations, and as such, fails to capture the full spectrum of clinical heterogeneity that characterizes the NF1 patient population.

To formally evaluate the potential impact of the germline NF1 gene mutation on optic glioma formation and growth, we performed proof-of-principle studies using *Nf1* GEM strains harboring two distinct NF1 patient-derived germline *Nf1* gene mutations. Herein, we demonstrate that mice harboring the R681X, but not the G848R, mutation develop optic gliomas. In addition, we show that the R681X mutation results in gliomas with greater microglia infiltration, tumor proliferation, and associated retinal ganglion cell loss relative to conventional knockout mice, revealing both cell-autonomous and stromal effects for the germline *Nf1* gene mutation on disease pathogenesis. Collectively, these data provide the first demonstration that the germline NF1 gene mutation is one important factor that underlies clinical heterogeneity relevant to risk assessment in this common neurogenetic condition.

Results

Neurofibromin expression is dictated by germline *Nf1* gene mutation

To establish the impact of the germline *Nf1* gene mutation on optic glioma formation, we leveraged GEM technology to engineer two distinct patient-derived NF1 gene mutations into C57BL/6 ES cells and generate mice harboring these germline mutations (Li K and Kesterson R, manuscript in preparation). The first line harbors a c.2542G>C missense mutation in exon 21 [Gly848Arg; G848R; (20)], while the second harbors a c.2041C>T nonsense mutation [Arg681*; R681X; (21)], causing a premature stop codon in exon 18 (Fig. 1A). Since murine *Nf1* optic glioma formation requires the coupling of somatic *Nf1* inactivation in neuroglial progenitors with a germline *Nf1* gene mutation (14,22), we employed the glial fibrillary acid protein (GFAP)-Cre strain to generate conditional *Nf1* knockout (CKO) mice (23) bearing each NF1-

patient germline *Nf1* gene mutation: *Nf1*^{flox/G848R}; GFAP-Cre (G848R^{CKO}) and *Nf1*^{flox/R681X}; GFAP-Cre (R681X^{CKO}) mice. All mice were maintained on a pure C57BL/6 genetic background. To determine whether neurofibromin expression was differentially impacted by these NF1 patient-derived germline *Nf1* gene mutations, G848R^{CKO}, neo^{CKO} and R681X^{CKO} mouse brainstem samples were analyzed by western blot. G848R^{CKO}, neo^{CKO} and R681X^{CKO} mice exhibited 38, 47 and 77% reductions in brainstem neurofibromin expression, respectively, relative to control mice (Fig. 1B). A similar pattern of neurofibromin expression was observed in the optic nerves from G848R^{CKO}, neo^{CKO} and R681X^{CKO} mice by immunohistochemistry (Fig. 1C).

Optic glioma formation is dependent on the germline *Nf1* gene mutation

Based on prior studies demonstrating that *Nf1*^{flox/neo}; GFAP-Cre CKO (neo^{CKO}) mice (harboring the neomycin knockout allele) develop optic gliomas with >95% penetrance by 3 months of age (16,24), G848R^{CKO} and R681X^{CKO} mice were aged to 3 months prior to optic nerve analysis. We analyzed a minimum of 12 mice per genotype in total. Whereas G848R^{CKO} mice had optic nerve volumes indistinguishable from controls, there was a 43% increase in optic nerve volumes from R681X^{CKO} mice (>95% penetrance by 3 months), similar to neo^{CKO} mice (48% increase; Fig. 2A). In addition, R681X^{CKO} mouse optic nerves had increased cellularity and atypical cells, histopathologic features similar to neo^{CKO} mouse optic gliomas. These features were not found in G848R^{CKO} mouse optic nerves (Fig. 2B). Immunostaining for GFAP, a marker of glial cells, revealed the highest level of immunoreactivity in the optic nerves of R681X^{CKO} mice, slightly greater than observed in neo^{CKO} mouse optic gliomas. Similarly, R681X^{CKO} optic nerves exhibited increased proliferation (%Ki67⁺ cells) compared with control and G848R^{CKO} mice (~14-fold increase) as well as to neo^{CKO} optic nerves (2.2-fold increase) (Fig. 2D).

One of the common morbidities seen in children with NF1-associated optic gliomas is reduced visual acuity (12,13) due to retinal ganglion cell (RGC) loss and retinal nerve fiber layer (RNFL) thinning (25). We used phospho-neurofilament heavy (pNF-H) chain immunohistochemistry as a surrogate marker of axonal injury in the optic nerve, based on previous studies in other models of nervous system injury (26,27). Increased pNF-H immunoreactivity was detected in the optic nerves from neo^{CKO} mice, which was further elevated with punctate staining in R681X^{CKO} mice (Fig. 3A). Consistent with the differential impact of the germline *Nf1* gene mutation on optic glioma formation and growth (proliferation), the retinae from R681X^{CKO} mice exhibited a 5.3-fold increase in TUNEL⁺ cells, a 3.2-fold reduction of Brn3a⁺ RGCs, and a 3.3-fold decrease in RNFL thickness relative to G848R^{CKO} and control mice (Fig. 3B). Importantly, there was a 1.5-fold increase in TUNEL⁺ cells, 27% reduction of Brn3a⁺ RGCs, and 1.78-fold decrease in RNFL thickness in R681X^{CKO} mice compared with neo^{CKO} mice (Fig. 3C). Together with the results described above, these data firmly demonstrate that neither the R681X nor the G848R mutation is equivalent to the conventional neomycin knockout allele, thus establishing differential effects of the germline *Nf1* gene mutation on optic glioma formation, growth, and associated RGC survival.

The differential impact of the germline *Nf1* gene mutation results from effects on both astrocytes and microglia

The differences observed between neo^{CKO}, G848R^{CKO} and R681X^{CKO} optic nerves could reflect changes in the levels of

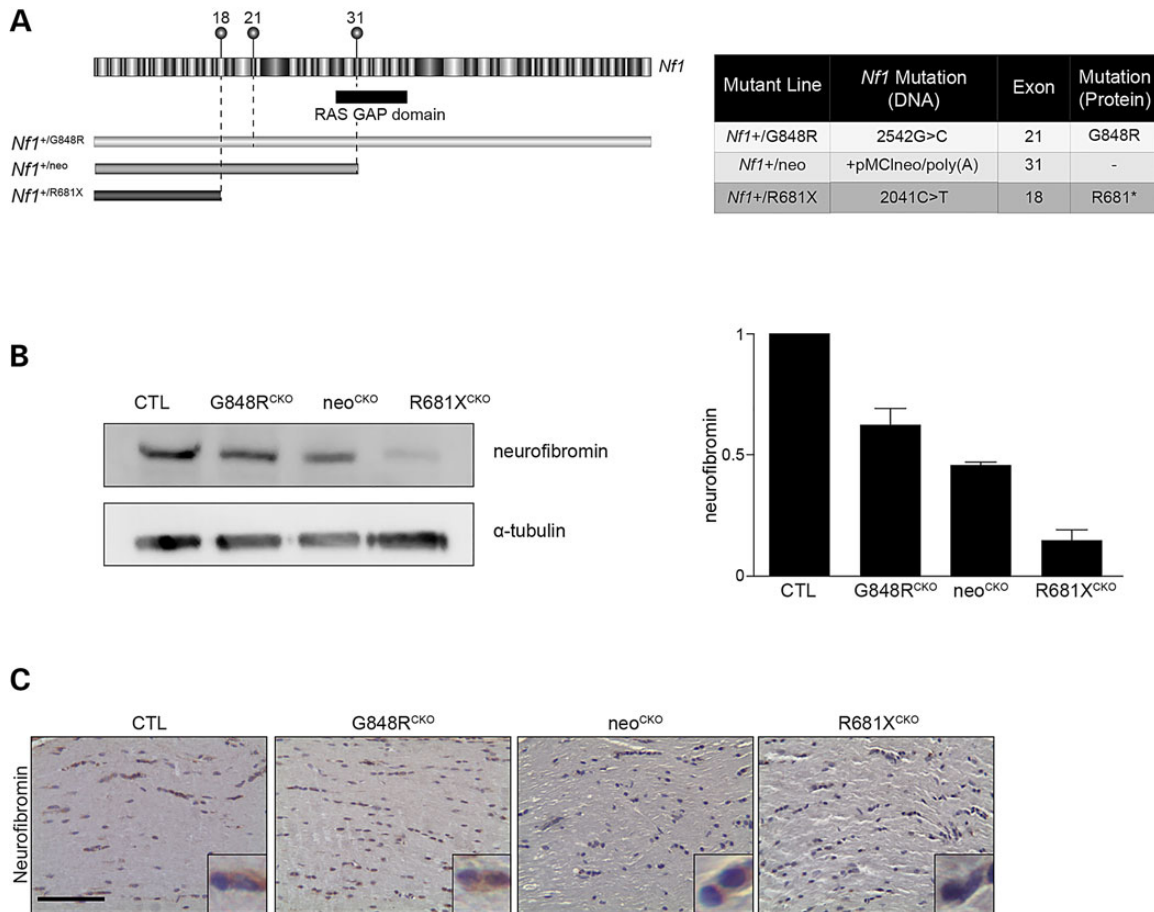


Figure 1. The germline *Nf1* gene mutation determines the level of neurofibromin expression. (A) Schematic illustration of the mouse *Nf1* gene, with the alternate exons and RAS-GAP domain indicated. The positions of the three germline *Nf1* gene mutations are depicted above exons 18, 21 and 31. (B) Neurofibromin expression was reduced in the brainstem of mice with Cre-mediated *Nf1*^{fllox} inactivation and G848R^{CKO} and R681X^{CKO} or null KO (neo^{CKO}) alleles by 38, 77 and 47%, respectively, relative to control mice following normalization to α -tubulin. (C) The effect of these germline *Nf1* gene mutations on neurofibromin expression was examined in the optic nerve by immunohistochemistry. At least three mice were used per genotype.

astrocyte hyperproliferation following somatic *Nf1* gene inactivation. To assess this potential effect, we analyzed brainstem astrocytes, since primary astrocyte cultures derived from murine optic nerves contain a heterogeneous population of macroglia (28) and the brainstem is the second most common brain region where gliomas arise in children with NF1 (29). As such, primary brainstem astrocytes were isolated from *Nf1*^{fllox/G848R}, *Nf1*^{fllox/neo} and *Nf1*^{fllox/R681X} mice and were infected with an adenovirus containing either Cre recombinase (Cre) to inactivate the *Nf1*^{fllox} allele or β -galactosidase (LacZ) to serve as controls. Importantly, the degree of neurofibromin reduction was similar between G848R, neo, and R681X astrocytes following Cre-mediated recombination of the *Nf1*^{fllox} allele relative to their respective controls (not shown), suggesting that any differences in proliferation observed using these three astrocyte populations reflected the contribution of the germline *Nf1* gene mutation. Following loss of the *Nf1*^{fllox} allele (Cre infection), we observed no significant increase in G848R^{CKO} astrocyte proliferation relative to *Nf1*^{fllox/fllox} controls, whereas neo^{CKO} and R681X^{CKO} astrocytes exhibited a 3.2–4-fold increase in proliferation (Fig. 4A).

We next examined the downstream signaling pathways hyperactivated following neurofibromin loss. For these studies, immunohistochemistry was employed to determine the percentage of cells in the murine optic nerves that exhibit AKT (phospho-

Akt^{Ser473}, pAkt^{Ser473}), ERK (phospho-ERK^{Thr202/Tyr204}, pERK^{Thr202/Tyr204}) and mTOR (phospho-S6^{Ser240/244}, pS6^{Ser240/244}) activation *in vivo*. This analysis revealed increased numbers of cells with neurofibromin downstream effector activation in neo^{CKO} (pAkt^{Ser473}, 9-fold increase, pERK^{Thr202/Tyr204}, 7.4-fold increase, pS6^{Ser240/244}, 2.8-fold increase) and R681X^{CKO} (pAkt^{Ser473}, 10.4-fold increase, pERK^{Thr202/Tyr204}, 7.1-fold increase, pS6^{Ser240/244}, 3.3-fold increase) mice compared with control and G848R^{CKO} mice (Fig. 4B–D). Collectively, these findings demonstrate that one mechanism by which the germline *Nf1* gene mutation dictates optic glioma formation and growth is by creating cell-autonomous differences in neurofibromin downstream effector activation and astrocyte proliferation *in vitro* and *in vivo*.

While this cell-autonomous effect of the germline *Nf1* gene mutation on astrocyte proliferation *in vitro* explains the ability of neo^{CKO} and R681X^{CKO}, but not G848R^{CKO}, mice to form optic gliomas, it does not account for the greater proliferation observed in R681X^{CKO} mice relative to neo^{CKO} mice *in vivo*. Previous studies from our laboratory have established an obligate role for non-neoplastic (stromal) cells in the formation and maintenance of murine optic gliomas (30–33). In particular, we have shown that brain microglia are required for optic glioma development and continued growth, such that silencing microglia function delays gliomagenesis and reduces optic glioma growth. Consistent with

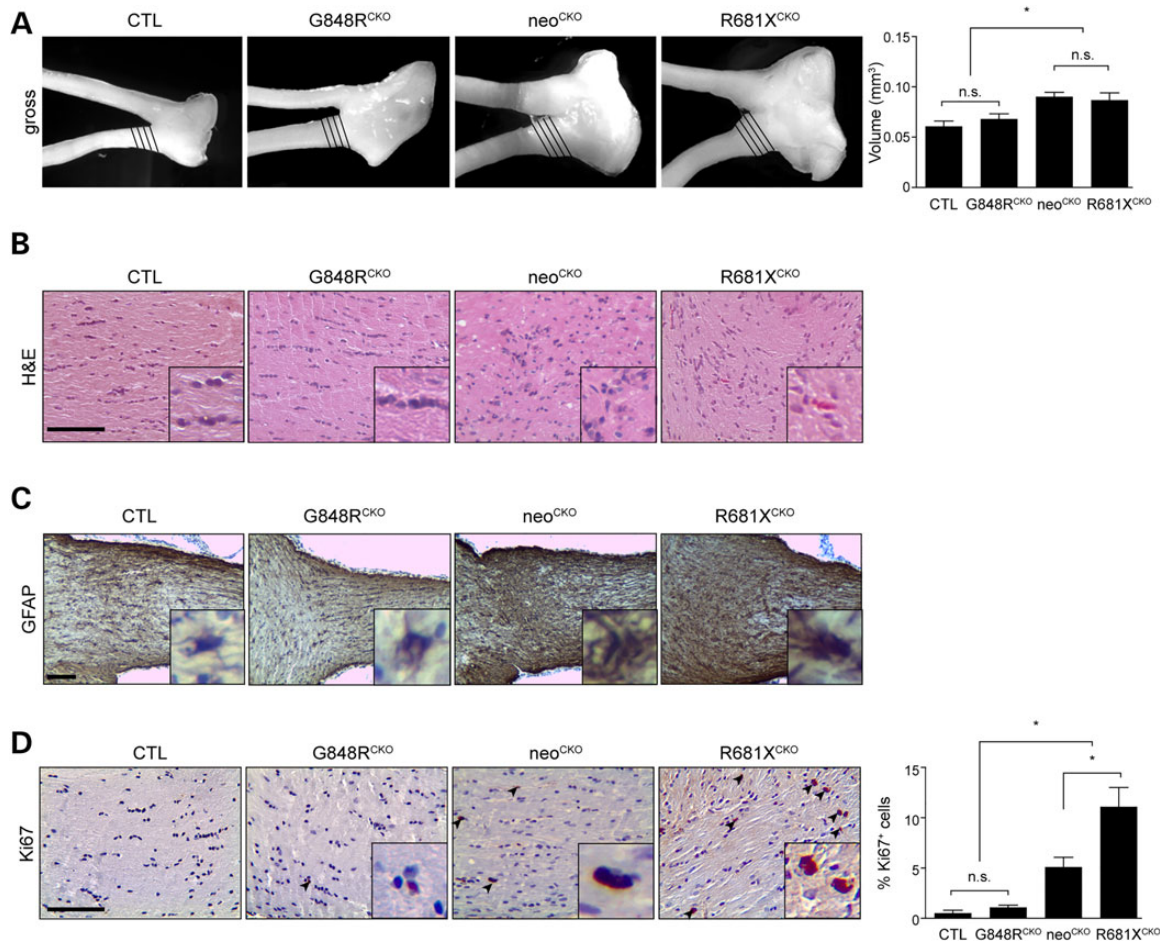


Figure 2. The germline *Nf1* gene mutation dictates optic glioma formation and proliferation. (A) Increased optic nerve volumes were observed in conditional knockout (neo^{CKO}) (1.49-fold) and R681X^{CKO} (1.43-fold) optic nerves relative to *Nf1*^{fl^{ox}/fl^{ox}} control littermates (CTL), while no significant changes were detected between G848R^{CKO} mice (mean = 0.07 ± 0.005 mm³) and controls (mean = 0.062 ± 0.005 mm³). (n = 6 mice per genotype). (B) Haematoxylin and eosin staining of the optic nerves revealed hypercellularity and nuclear atypia in neo^{CKO} and R681X^{CKO} optic nerves (n = 6 mice per genotype). (C) Increased GFAP immunoreactivity is observed in neo^{CKO} and R681X^{CKO} compared with no increase seen between G848R^{CKO} and controls. (D) R681X^{CKO} mice exhibited increased Ki67 immunoreactivity (14-fold; 2.2-fold) compared with control and neo^{CKO} mice, respectively (n = 5 mice per genotype). Scale bars: 100 μm. All data are represented as means ± s.e.m. (*P < 0.05; one-way ANOVA with Bonferroni post-test).

a critical role for microglia in these brain tumors, there were 2-fold more microglia in R681X^{CKO} compared with neo^{CKO} mouse optic nerves (Fig. 5A).

To determine whether this increase in microglia explains the higher levels of proliferation observed in R681X^{CKO} mouse optic gliomas, we focused on microglia-mediated paracrine effects. First, we examined JNK activation (JNK^{Thr183/Tyr185}; pJNK), based on our previous finding that *Nf1*^{+/-} microglia have increased levels of JNK activation *in vitro* and that pharmacological JNK inhibition reduces *Nf1* mouse optic glioma proliferation *in vivo* (33). Consistent with increased microglia functional activity, optic gliomas from R681X^{CKO} mice had a 2.4-fold greater percentage of pJNK⁺ cells relative to neo^{CKO} mice (Fig. 5B). It is important to note that the JNK activity (pJNK) was localized to Iba1⁺ microglia (Fig. 5C). Second, since microglia promote glioma growth through the elaboration of specific chemokines, like Ccl5 (34), we next quantified the percentage of Ccl5⁺ cells in these optic nerves, and observed a 1.9-fold greater percentage of Ccl5⁺ cells in R681X^{CKO} relative to neo^{CKO} optic gliomas (Fig. 5D). Third, Ccl5 can activate phosphoinositol-3-kinase (35–37), leading to Akt^{Thr308} phosphorylation (Akt^{Thr308}) (38). As such, increased AKT^{Thr308} phosphorylation (2.9-fold) was only observed in the

optic nerves from R681X^{CKO} mice relative to controls (Fig. 5E). Moreover, Akt^{Thr308} activation was localized to astrocytes, as revealed by GFAP/pAKT^{Thr308} double labeling (data not shown). Together, these data reveal both cell-intrinsic (astrocyte) and non-cell-intrinsic (microglia) mechanisms by which the germline *Nf1* gene mutation differentially dictates optic glioma formation and growth (Fig. 6).

Discussion

Little is known about the factors that underlie the significant clinical heterogeneity that characterizes many human monogenic diseases. Using NF1 as an instructive model of a common monogenic disorder, we sought to critically evaluate the differential impact of the germline NF1 gene mutation on optic glioma formation. With over 1300 different germline NF1 gene mutations documented and few recurrent mutations (39), robust correlations between germline mutations and clinical features have been largely unsuccessful (2,40). Nonetheless, several intriguing genotype–phenotype correlations have been reported (4–6,41). In addition, recent work from our laboratory employing NF1-patient-derived iPSCs with different germline NF1 gene mutations

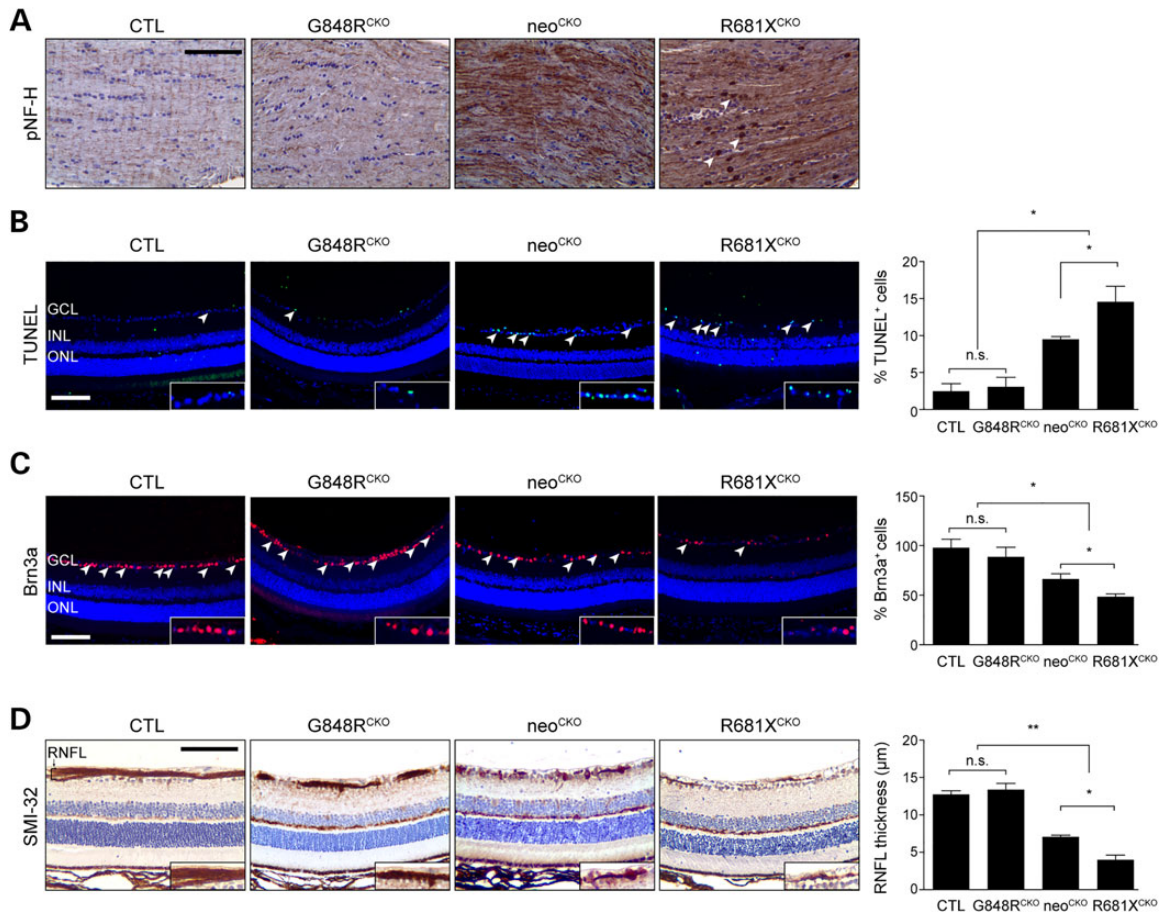


Figure 3. The germline *Nf1* gene mutation dictates the degree of optic glioma-induced retinal dysfunction. (A) pNF-H immunostaining in the optic nerves of control, G848R^{CKO}, neo^{CKO} and R681X^{CKO} mice revealed increased immunoreactivity in neo^{CKO} and R681X^{CKO} mice, with R681X^{CKO} mice exhibiting additional punctate staining (arrowheads). (B) The retinæ of R681X^{CKO} and neo^{CKO} mice had increased percentages of TUNEL⁺ cells (5.9- and 4.8-fold increase, respectively) compared with control mice ($n = 5$ mice per genotype). (C) The retinæ of R681X^{CKO} and neo^{CKO} mice had lower percentages of Brn3a⁺ cells (50 and 41% decrease, respectively) compared with control mice ($n = 5$ mice per genotype). (D) The retinæ of R681X^{CKO} and neo^{CKO} mice had RNFL thinning as revealed by SMI-32 immunostaining (3.4- and 3.2-fold decrease, respectively) compared with control mice ($n = 5$ mice per genotype). GCL, ganglion cell layer; INL, inner nuclear layer; ONL, outer nuclear layer; RNFL, retinal nerve fiber layer. Scale bars: 100 μm . All data are represented as means \pm s.e.m. (** $P < 0.01$; * $P < 0.05$; one-way ANOVA with Bonferroni post-test). n.s., not significant.

has revealed differences in neurofibromin expression and downstream signaling (9). However, since these iPSCs harbor different genomic backgrounds, which could also influence neurofibromin levels and function, we sought to formally evaluate the impact of the germline *NF1* gene mutation engineered in mice on the identical genetic background.

For these proof-of-principle studies, two GEM strains were engineered to harbor germline *Nf1* gene mutations most representative of the types of mutations found in individuals with NF1: nonsense (R681X) and missense (G848R) mutations (9,42). For the first time, we demonstrate distinct effects of two different germline *NF1* gene mutations on murine optic glioma formation, growth, and associated retinal pathology. Herein, we show that *Nf1* mutant mice harboring the R681X, but not the G848R, germline *Nf1* gene mutation develop optic gliomas characterized by higher proliferative indices, increased GFAP immunoreactivity, and greater microglial infiltration. In addition, we demonstrate that these mutations are different from the conventional *Nf1* knockout allele in terms of disease severity, revealing both cell-autonomous and non-cell-autonomous (stromal) mechanisms. Collectively, these novel findings argue that the germline *NF1* gene mutation is one important factor in dictating disease pathogenesis.

It is interesting to note that the two germline *Nf1* gene mutations have distinct effects on neurofibromin expression *in vivo*. The G848R missense mutation results in <38% reduction of neurofibromin levels, whereas the R681X nonsense mutation confers >77% reduction. These findings are similar to the neurofibromin expression profiles observed in NF1 patient-derived fibroblasts and iPSC-NPs, where patients clustered into two subgroups based on neurofibromin expression: Group 1 with minor reductions (<25%) and Group 2 with >70% reduced expression (9). Importantly, neurofibromin expression in the neomycin KO (neo^{CKO}) mouse is reduced by ~50%. Further underscoring the inability of current GEM models to fully capture the impact of patient mutation-driven phenotypes, optic nerve gliomas developing in mice harboring the nonsense R681X mutation (R681X^{CKO}) were more aggressive than those developing in neo^{CKO} mice (more microglia and increased proliferative indices).

These findings echo similar experiences in modeling other genetic conditions. For example, mice with a targeted disruption of the *N*-acetylglucosamine-1-phosphotransferase (*GNPTAB*) gene lack some of the characteristic features seen in patients with mucopolipidosis II (MLII) (43), whereas mice engineered with a patient MLII *GNPTAB* mutation show facial and skeletal anomalies, lysosomal malfunction and reduced lifespan (44). In

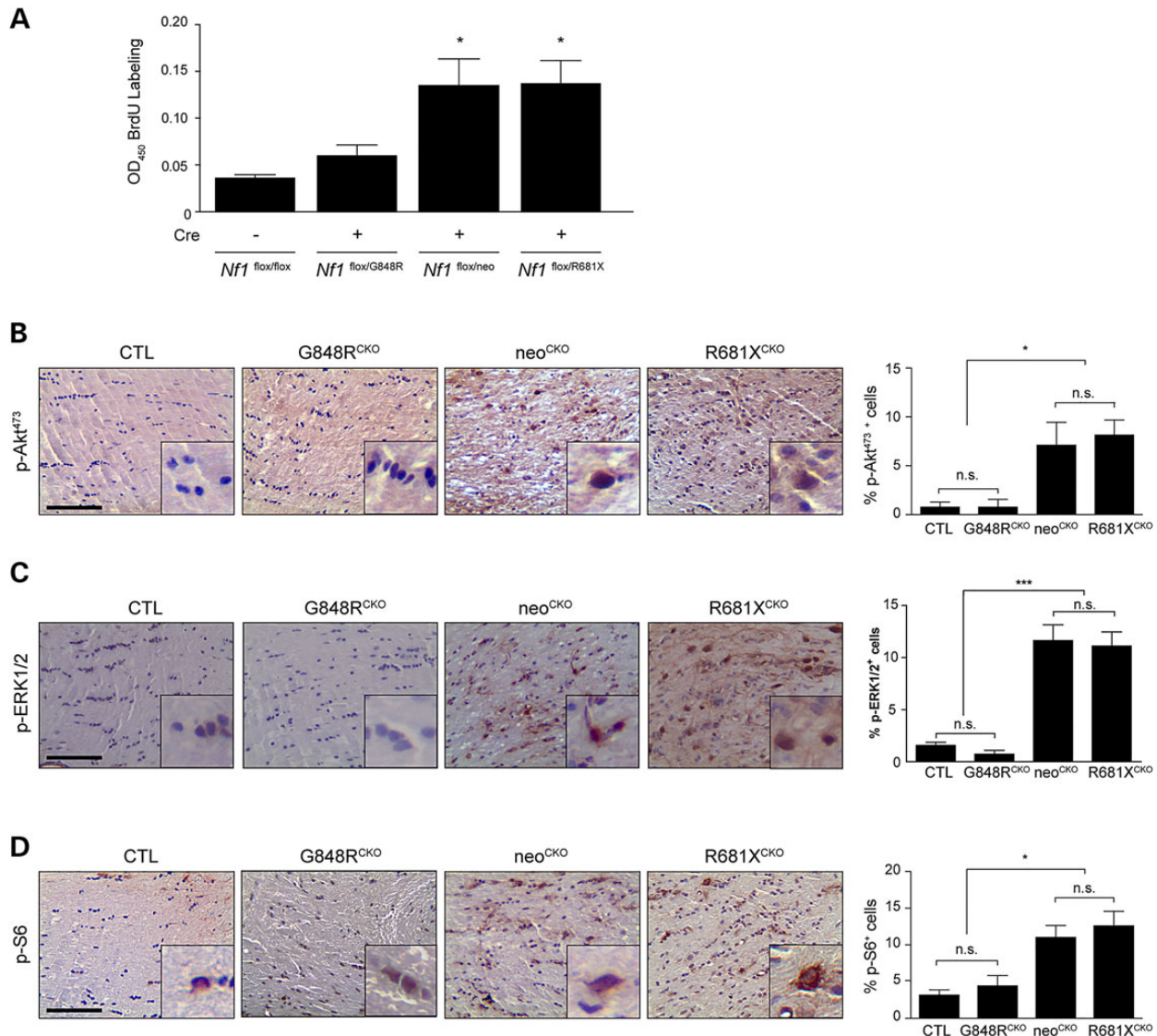


Figure 4. Optic glioma formation and growth is partly determined by the effect of the germline *Nf1* gene mutation on astrocyte RAS effector activation and proliferation. (A) Astrocyte proliferation was increased by 3.2- to 4.0-fold following Cre-mediated *Nf1*^{flox} inactivation (Cre) in *Nf1*^{G681X/flox} and *Nf1*^{neo/flox} astrocytes, but only by 1.3-fold in *Nf1*^{G848R/flox} astrocytes. Normalization is relative to control *Nf1*^{flox/flox} astrocytes (LacZ infection) ($n > 3$ samples per genotype). Data are represented as means \pm s.e.m. ($^*P < 0.05$; one-way ANOVA with Dunn's multiple comparison test). Immunostaining with pAkt^{Ser473} (B) pERK^{Thr202/Tyr204} (C) and pS6^{Ser240/244} (D) antibodies revealed a greater percentage of pAkt^{Ser473}, pERK^{Thr202/Tyr204} and pS6^{Ser240/244}-immunoreactive cells in the optic nerves of neo^{CKO} (pAkt^{Ser473}: 9-fold increase, pERK^{Thr202/Tyr204}: 7.4-fold increase, pS6^{Ser240/244}: 2.8-fold increase) and R681X^{CKO} (pAkt^{Ser473}: 10.4-fold increase, pERK^{Thr202/Tyr204}: 7.1-fold increase, pS6^{Ser240/244}: 3.3-fold increase) optic nerves relative to *Nf1*^{flox/flox} littermate controls (CTL). A minimum of four animals per genotype was assayed. n.s., not significant. Scale bars: 100 μ m. Data are represented as means \pm s.e.m. ($^*P < 0.05$, $^{***}P < .001$; one-way ANOVA with Bonferroni post-test).

addition, mice with constitutively active oncogenic KRAS^{G12D} mutations fail to develop cardiomyopathy, a common feature of Noonan Syndrome (45), whereas GEM models harboring the recurrent patient-derived KRAS^{+V141} mutation exhibit the characteristic growth, craniofacial, and cardiac defects associated with the human disease (46).

Moreover, we demonstrate that the specific germline *NF1* gene mutation differentially impacts on optic glioma severity in at least two distinct ways. In this regard, we report both cell-autonomous and stromal (non-cell-autonomous) effects of the germline *NF1* gene mutation on disease pathogenesis *in vitro* and *in vivo*. The cell-autonomous effect on optic glioma results from the effect of reduced neurofibromin expression on the downstream effector pathways most critical for mediating tumor growth. Previous

studies from our laboratory and others have shown that loss of neurofibromin function results in increased ERK and AKT activation, which each converge on mTOR to drive *Nf1*-deficient astrocyte proliferation *in vitro* and *Nf1* optic glioma growth *in vivo* (16,47–49). In the current report, loss of the *Nf1*^{flox} allele by Cre-mediated excision had more significant effects on astrocyte proliferation when coupled with the neo or R681X germline *Nf1* gene mutation than the G848R mutation *in vitro*. Similarly, in the optic nerves *in vivo*, greater numbers of cells with increased ERK (phospho-ERK^{Thr202/Tyr204}), AKT (phospho-Akt^{Ser473}), and mTOR (phospho-S6^{Ser240/244}) activation were observed in neo^{CKO} and R681X^{CKO} mice relative to G848R^{CKO} and control mice, which were indistinguishable from each other. Studies are underway to more precisely define how the different germline *Nf1* gene mutations

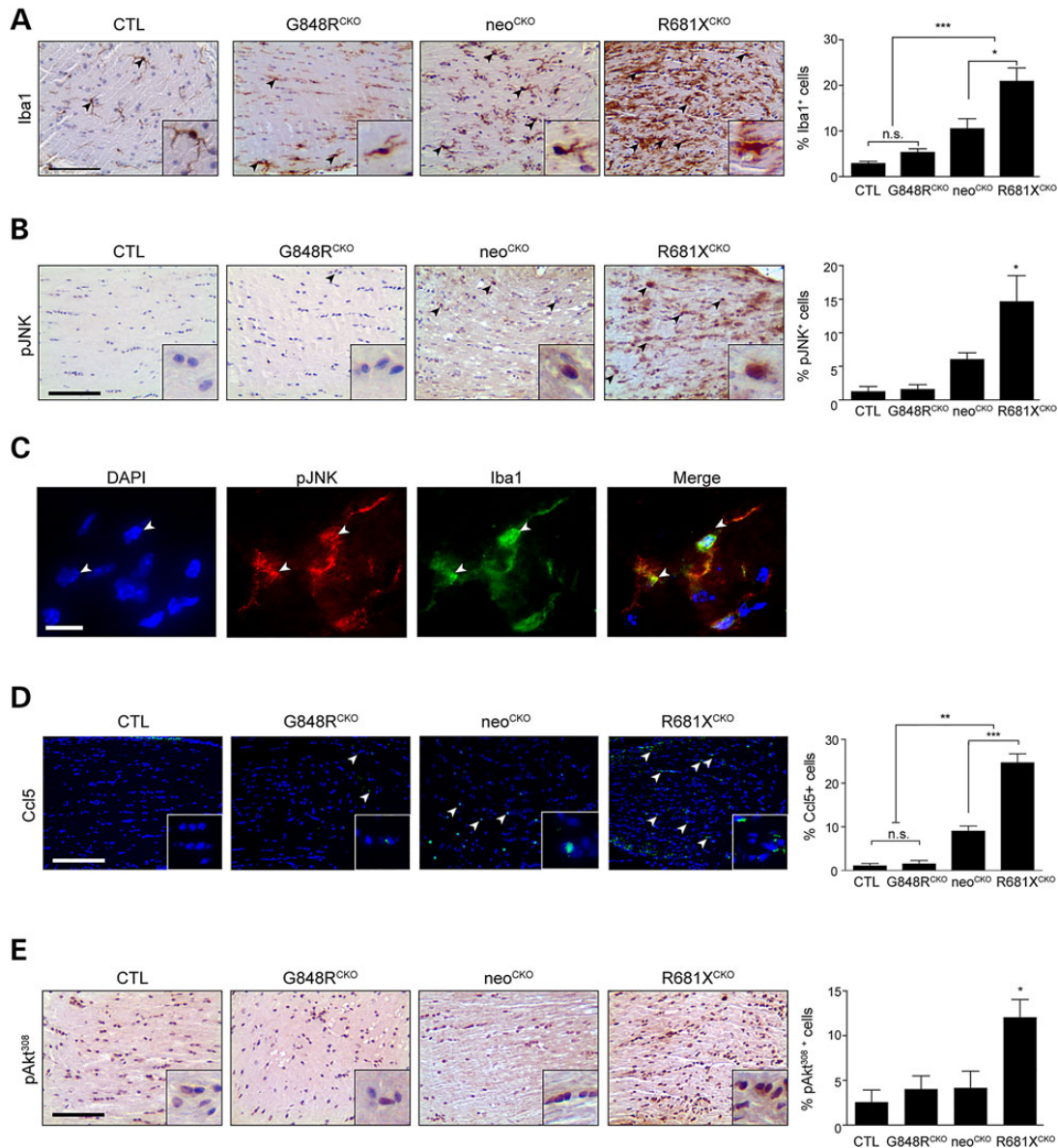


Figure 5. Optic glioma formation and growth is partly determined by the effect of the germline *Nf1* gene mutation on microglia number and function. (A) Iba1 immunostaining demonstrates increased numbers of microglia in the optic nerves of neo^{CKO} (3.6-fold) and R681X^{CKO} (7.1-fold) mice relative to controls (CTL). Whereas R681X^{CKO} mice have more microglia than neo^{CKO} mice (2-fold), no increase in microglia numbers was detected in G848R^{CKO} mice relative to controls ($n = 5$ mice per genotype). (B) Increased percentages of pJNK⁺ cells were observed in neo^{CKO} (4.66-fold) and R681X^{CKO} (11.28-fold) optic nerves relative to control optic nerves ($n = 4$ mice per genotype). (C) Immunofluorescence revealing pJNK staining in Iba1⁺ cells (microglia) within the optic nerves of R681X^{CKO} mice. White arrowheads depict two independent cells positively labeled with both pJNK and Iba1. (D) Increased percentages of CCL5⁺ cells were observed in neo^{CKO} (14.56-fold) and R681X^{CKO} (27.37-fold) optic nerves compared with control mice ($n = 5$ mice per genotype). (E) A greater percentage of pAkt^{Thr308}-immunoreactive cells was found in R681X^{CKO} mice relative to control (4.68-fold), and neo^{CKO} (2.88-fold) optic nerves ($n = 4$ mice per genotype). Scale bars: 100 μ m. All data are represented as means \pm s.e.m. (** $P < 0.001$; ** $P < 0.01$; * $P < 0.05$; one-way ANOVA with Bonferroni post-test).

impact on neurofibromin-regulated effector pathway activation in response to specific growth factors present in these optic gliomas.

In addition, there was a non-cell-autonomous (stromal) effect that reflected the impact of the germline *NF1* gene mutation on non-neoplastic cells in the tumor microenvironment (microglia). Microglia are brain tissue macrophages that promote optic glioma development and growth in *Nf1* GEM strains. These immune system-like cells alter their function in response to changes in *Nf1* gene expression, such that *Nf1*^{+/*neo*} microglia exhibit increased JNK activation (33). Consistent with the importance of microglial JNK hyperactivation in stroma-mediated glioma

growth, pharmacologic JNK inhibition reduces *Nf1* optic glioma proliferation *in vivo*. As such, optic gliomas in R681X^{CKO} mice had greater numbers of phospho-JNK-immunoreactive microglia and increased microglial expression of Ccl5, a chemokine recently shown to maintain murine optic glioma growth *in vivo* (34). In these latter studies, Ccl5 was sufficient to increase *Nf1*-deficient optic nerve astrocyte growth *in vitro* and treatment with Ccl5 neutralizing antibodies reduced optic glioma growth *in vivo*. While the precise mechanism responsible for microglial Ccl5-mediated astrocyte hyperproliferation is still under investigation, increased Ccl5 expression in the tumor is most likely to drive

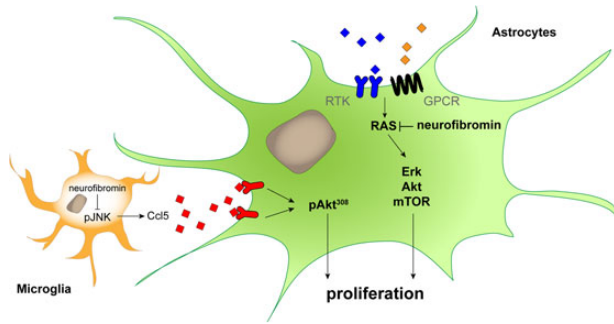


Figure 6. The germline *Nf1* gene mutation independently determines astrocyte and microglia dysfunction relative to optic glioma formation and growth. Proposed model of the cell-autonomous (astrocytes) and non-cell-autonomous (microglia) effects of the germline *Nf1* gene mutation on murine optic glioma growth. In microglia, the germline *Nf1* gene mutation differentially impacts on JNK activation and Ccl5 expression, which results in varying levels of chemokine (Ccl5)-mediated Akt^{Thr308} activation in neoplastic astrocytes to increase optic glioma growth *in vivo*. Similarly, the germline *Nf1* gene mutation differentially determines neurofibromin-regulated downstream signaling pathway activation and glial cell proliferation, leading to differing levels of cell-intrinsic astrocyte growth in the tumor.

astroglial cell proliferation through Akt^{Thr308} hyperactivation, as observed in other cancers (35–37). Current work is focused on determining how growth factors, like Ccl5, elaborated by cells in the tumor microenvironment regulate *Nf1* optic glioma growth relevant to the development and evaluation of future stroma-directed brain tumor therapies.

In summary, the proof-of-concept studies presented in this report provide the first evidence for a clear effect of the germline *Nf1* gene mutation on disease pathogenesis in NF1. Combined with other risk factors, such as genomic single nucleotide polymorphisms (50) and patient sex (51,52), further investigations using similar strains with different germline *Nf1* gene mutations found in people with NF1, specifically those with particular clinical phenotypes (e.g. p1809) may yield critical new insights into the impact of the germline mutation on other medical issues affecting children and adults with NF1. Together with preliminary findings using NF1 patient-derived iPSCs and NPs, these murine studies raise the intriguing possibility that identifying the germline NF1 gene mutation may have some predictive utility in this at-risk patient population.

Materials and Methods

Mice

All animals were maintained on an inbred C57BL/6 background using a 12 h light–dark cycle with *ad libitum* access to food and water. Heterozygous *Nf1* mice were generated with one wild-type copy of the *Nf1* gene and one copy containing either a missense mutation in exon 21 (corresponding to the human c.2542G>C NF1 gene mutation; Gly848Arg, p.G848R) (Li and Kesterson, manuscript in preparation; draft readily available to reviewers upon request), a nonsense mutation in exon 18 (corresponding to the human c.2041C>T NF1 gene mutation; Arg681*, p.R681) (Li and Kesterson, manuscript in preparation; draft readily available to reviewers upon request) or a null inactivating allele created by the insertion of a neomycin cassette into exon 31 (*Nf1*^{+/neo}) (19). G848R and R681X mice were generated using C57BL/6 ES cells and backcrossed a minimum of 10 times to wild-type C57BL/6 mice, while neo31 mice have been extensively backcrossed onto the C57BL/6 genetic background for

over 15 years in the laboratory. Conditional knockout mice were generated with the G848R, neo31 or R681X mutation as the germline *Nf1* allele, with somatic *Nf1* gene inactivation resulting from Cre-mediated excision of the *Nf1*^{lox} allele in neuroglial progenitor cells (22). The resulting strains included *Nf1*^{lox/G848R}, GFAP-Cre (G848R^{CKO}), *Nf1*^{lox/neo}; GFAP-Cre (neo^{CKO}) (14) and *Nf1*^{lox/R681X}, GFAP-Cre (R681X^{CKO}). Littermate *Nf1*^{+/+} and *Nf1*^{lox/lox} (FF) mice were used as controls. All experiments were performed on 3-month-old animals, unless otherwise stated, under active Animal Studies Committee protocols at Washington University. Mice were randomly assigned to all experimental groups without bias, and the investigators were blinded to sample group allocation and subsequent analysis during all of the experiments.

Optic nerve volume measurements

Optic nerves with an intact chiasm were microdissected following transcardial perfusion. Optic nerves were photographed and diameters were measured at the chiasm (150, 300 and 450 μ m anterior to the chiasm) to generate optic nerve volumes (16). A minimum of six animals per genotype were employed for these experiments.

Retinal nerve fiber layer measurements

RNFL thickness was quantitated using the average of 15 measurements of SMI-32-stained axons 0–250 μ m proximal to the optic nerve head (ImageJ software) (53). A minimum of five animals per genotype were used for these experiments.

Western blotting, immunohistochemistry and immunofluorescence

Western blotting was performed on snap-frozen hippocampi or WBC pellets, lysed in RIPA buffer supplemented with protease inhibitors using appropriate primary antibodies (Supplementary Material, Table S1), secondary horseradish peroxidase-conjugated antibodies (Sigma) and ECL (Fisher) chemiluminescence (24). Western signal band intensity was quantified using ImageJ Software (National Institutes of Health, USA, <http://imagej.nih.gov/ij> Java 1.7.0_67). The western blot images illustrated are representative of separate sets of blots performed on a minimum of 10 independent animals per genotype. Quantitative data were obtained from analysis of all individual western blots. Immunohistochemistry and immunofluorescence were performed as previously described (54), on mice transcardially perfused with 4% PFA (Sigma) in 0.1 M sodium phosphate buffer (pH 7.4) and post-fixed in 4% PFA prior to paraffin embedding. For some immunofluorescence experiments (Brn3a, Ccl5), antibody signal amplification was performed using the TSA Cy3 Plus system (Perkin Elmer) (53). Four to 6 animals per genotype were used for these experiments.

Primary astrocyte culture and proliferation assay

Primary astrocytes were generated from the brainstems of postnatal Days 0–1 mouse pups and maintained in astrocyte growth medium (Dulbecco's modified Eagle's medium (DMEM) containing 10% fetal bovine serum and 1% penicillin/streptomycin) (53). To inactivate the conditional *Nf1*^{lox} allele, astrocytes (passage 1) were infected with adenovirus type 5 (Ad5) containing Cre recombinase (Ad5-Cre) (University of Iowa Gene Transfer Vector Core, Iowa City, IA, USA). Control infections employed Ad5 containing β -galactosidase (Ad5-LacZ). 4 days post-infection, astrocytes were passaged and serum starved for 48 h prior to western blotting and

proliferation analysis. Astrocyte proliferation was assessed using the BrdU Cell Proliferation ELISA kit (Roche) following manufacturer's instructions. Briefly, 6000 serum-starved astrocytes were labeled with BrdU for 18 h followed by 2-h incubation in peroxidase-conjugated anti-BrdU antibody. Proliferating astrocytes were identified using a colorimetric substrate reaction measured at 450 nm on a spectrophotometer (Bio-Rad). A minimum of six animals per genotype were used for each experiment, and these studies were replicated at least four independent times.

Statistical analyses

All statistical analyses were performed using GraphPad Prism 5 software (GraphPad Software). One- or two-way ANOVA with Bonferroni post-test correction analyses were employed for multiple comparisons.

Supplementary Material

Supplementary Material is available at HMG online.

Conflict of Interest statement. None declared.

Funding

J.A.T. was supported on the Vision Sciences (5-T32-EY13360) and Neuroscience (5-T32-NS007205-33) T32 training grants. These studies were funded by grants from the National Cancer Institute (1R01-CA195692-01) and Alex's Lemonade Stand Foundation to D.H.G.

References

- Jett, K. and Friedman, J.M. (2010) Clinical and genetic aspects of neurofibromatosis 1. *Genet. Med.*, **12**, 1–11.
- Szudek, J., Joe, H. and Friedman, J.M. (2002) Analysis of intra-familial phenotypic variation in neurofibromatosis 1 (NF1). *Genet. Epidemiol.*, **23**, 150–164.
- Friedman, J.M. (1999) Epidemiology of neurofibromatosis type 1. *Am. J. Med. Genet.*, **89**, 1–6.
- Bolcekova, A., Nemethova, M., Zatkova, A., Hlinkova, K., Pozgayova, S., Hlavata, A., Kadasi, L., Durovcikova, D., Gerinec, A., Husakova, K. et al. (2013) Clustering of mutations in the 5' ter-tile of the NF1 gene in Slovakia patients with optic pathway glioma. *Neoplasma*, **60**, 655–665.
- Sharif, S., Upadhyaya, M., Ferner, R., Majounie, E., Shenton, A., Baser, M., Thakker, N. and Evans, D.G. (2011) A molecular analysis of individuals with neurofibromatosis type 1 (NF1) and optic pathway gliomas (OPGs), and an assessment of genotype-phenotype correlations. *J. Med. Genet.*, **48**, 256–260.
- Upadhyaya, M., Huson, S.M., Davies, M., Thomas, N., Chuzhanova, N., Giovannini, S., Evans, D.G., Howard, E., Kerr, B., Griffiths, S. et al. (2007) An absence of cutaneous neurofibromas associated with a 3-bp inframe deletion in exon 17 of the NF1 gene (c.2970-2972 delAAT): evidence of a clinically significant NF1 genotype-phenotype correlation. *Am. J. Hum. Genet.*, **80**, 140–151.
- Pinna, V., Lanari, V., Daniele, P., Consoli, F., Agolini, E., Margiotti, K., Bottillo, I., Torrente, I., Bruselles, A., Fusilli, C. et al. (2015) p.Arg1809Cys substitution in neurofibromin is associated with a distinctive NF1 phenotype without neurofibromas. *Eur. J. Hum. Genet.*, **23**, 1068–1071.
- De Raedt, T., Brems, H., Wolkenstein, P., Vidaud, D., Pilotti, S., Perrone, F., Mautner, V., Frahm, S., Sciort, R. and Legius, E. (2003) Elevated risk for MPNST in NF1 microdeletion patients. *Am. J. Hum. Genet.*, **72**, 1288–1292.
- Anastasaki, C., Woo, A.S., Messiaen, L.M. and Gutmann, D.H. (2015) Elucidating the impact of neurofibromatosis-1 germline mutations on neurofibromin function and dopamine-based learning. *Hum. Mol. Genet.*, **24**, 3518–3528.
- Listernick, R., Charrow, J., Greenwald, M.J. and Esterly, N.B. (1989) Optic gliomas in children with neurofibromatosis type 1. *J. Pediatr.*, **114**, 788–792.
- Louis, D.N., Ohgaki, H., Wiestler, O.D., Cavenee, W.K., Burger, P.C., Jouvett, A., Scheithauer, B.W. and Kleihues, P. (2007) The 2007 WHO classification of tumours of the central nervous system. *Acta Neuropathol.*, **114**, 97–109.
- Fisher, M.J., Loguidice, M., Gutmann, D.H., Listernick, R., Ferner, R.E., Ullrich, N.J., Packer, R.J., Tabori, U., Hoffman, R.O., Arden-Holmes, S.L. et al. (2012) Visual outcomes in children with neurofibromatosis type 1-associated optic pathway glioma following chemotherapy: a multicenter retrospective analysis. *Neuro. Oncol.*, **14**, 790–797.
- Listernick, R., Ferner, R.E., Liu, G.T. and Gutmann, D.H. (2007) Optic pathway gliomas in neurofibromatosis-1: controversies and recommendations. *Ann. Neurol.*, **61**, 189–198.
- Bajenaru, M.L., Hernandez, M.R., Perry, A., Zhu, Y., Parada, L.F., Garbow, J.R. and Gutmann, D.H. (2003) Optic nerve glioma in mice requires astrocyte Nf1 gene inactivation and Nf1 brain heterozygosity. *Cancer Res.*, **63**, 8573–8577.
- Hegedus, B., Hughes, F.W., Garbow, J.R., Gianino, S., Banerjee, D., Kim, K., Ellisman, M.H., Brantley, M.A. Jr. and Gutmann, D.H. (2009) Optic nerve dysfunction in a mouse model of neurofibromatosis-1 optic glioma. *J. Neuropathol. Exp. Neurol.*, **68**, 542–551.
- Hegedus, B., Banerjee, D., Yeh, T.H., Rothermich, S., Perry, A., Rubin, J.B., Garbow, J.R. and Gutmann, D.H. (2008) Preclinical cancer therapy in a mouse model of neurofibromatosis-1 optic glioma. *Cancer Res.*, **68**, 1520–1528.
- Kaul, A., Toonen, J.A., Cimino, P.J., Gianino, S.M. and Gutmann, D.H. (2015) Akt- or MEK-mediated mTOR inhibition suppresses Nf1 optic glioma growth. *Neuro. Oncol.*, **17**, 843–853.
- Jacks, T., Shih, T.S., Schmitt, E.M., Bronson, R.T., Bernards, A. and Weinberg, R.A. (1994) Tumour predisposition in mice heterozygous for a targeted mutation in Nf1. *Nat. Genet.*, **7**, 353–361.
- Brannan, C.I., Perkins, A.S., Vogel, K.S., Ratner, N., Nordlund, M.L., Reid, S.W., Buchberg, A.M., Jenkins, N.A., Parada, L.F. and Copeland, N.G. (1994) Targeted disruption of the neurofibromatosis type-1 gene leads to developmental abnormalities in heart and various neural crest-derived tissues. *Genes Dev.*, **8**, 1019–1029.
- Pascual-Castroviejo, I., Pascual-Pascual, S.I., Velazquez-Fraqua, R., Botella, P. and Viano, J. (2007) Familial spinal neurofibromatosis. *Neuropediatrics*, **38**, 105–108.
- Kocova, M., Kochova, E. and Sukarova-Angelovska, E. (2015) Optic glioma and precocious puberty in a girl with neurofibromatosis type 1 carrying an R681X mutation of NF1: case report and review of the literature. *BMC Endocr. Disord.*, **15**, 82.
- Bajenaru, M.L., Zhu, Y., Hedrick, N.M., Donahoe, J., Parada, L.F. and Gutmann, D.H. (2002) Astrocyte-specific inactivation of the neurofibromatosis 1 gene (NF1) is insufficient for astrocytoma formation. *Mol. Cell. Biol.*, **22**, 5100–5113.
- Zhu, Y., Romero, M.I., Ghosh, P., Ye, Z., Charnay, P., Rushing, E.J., Marth, J.D. and Parada, L.F. (2001) Ablation of NF1 function in neurons induces abnormal development of cerebral cortex and reactive gliosis in the brain. *Genes Dev.*, **15**, 859–876.

24. Bajenaru, M.L., Garbow, J.R., Perry, A., Hernandez, M.R. and Gutmann, D.H. (2005) Natural history of neurofibromatosis 1-associated optic nerve glioma in mice. *Ann. Neurol.*, **57**, 119–127.
25. Avery, R.A., Liu, G.T., Fisher, M.J., Quinn, G.E., Belasco, J.B., Phillips, P.C., Maguire, M.G. and Balcer, L.J. (2011) Retinal nerve fiber layer thickness in children with optic pathway gliomas. *Am. J. Ophthalmol.*, **151**, 542–549 e542.
26. Rosenfeld, J., Dorman, M.E., Griffin, J.W., Gold, B.G., Sternberger, L.A., Sternberger, N.H. and Price, D.L. (1987) Distribution of neurofilament antigens after axonal injury. *J. Neuropathol. Exp. Neurol.*, **46**, 269–282.
27. Parrilla-Reverter, G., Agudo, M., Nadal-Nicolas, F., Alarcon-Martinez, L., Jimenez-Lopez, M., Salinas-Navarro, M., Sobrado-Calvo, P., Bernal-Garro, J.M., Villegas-Perez, M.P. and Vidal-Sanz, M. (2009) Time-course of the retinal nerve fibre layer degeneration after complete intra-orbital optic nerve transection or crush: a comparative study. *Vis. Res.*, **49**, 2808–2825.
28. Solga, A.C., Gianino, S.M. and Gutmann, D.H. (2014) NG2-cells are not the cell of origin for murine neurofibromatosis-1 (NF1) optic glioma. *Oncogene*, **33**, 289–299.
29. Guillamo, J.S., Creange, A., Kalifa, C., Grill, J., Rodriguez, D., Doz, F., Barbarot, S., Zerah, M., Sanson, M., Bastuji-Garin, S. et al. (2003) Prognostic factors of CNS tumours in Neurofibromatosis 1 (NF1): a retrospective study of 104 patients. *Brain*, **126**, 152–160.
30. Daginakatte, G.C. and Gutmann, D.H. (2007) Neurofibromatosis-1 (NF1) heterozygous brain microglia elaborate paracrine factors that promote Nf1-deficient astrocyte and glioma growth. *Hum. Mol. Genet.*, **16**, 1098–1112.
31. Pong, W.W., Higer, S.B., Gianino, S.M., Emnett, R.J. and Gutmann, D.H. (2013) Reduced microglial CX3CR1 expression delays neurofibromatosis-1 glioma formation. *Ann. Neurol.*, **73**, 303–308.
32. Simmons, G.W., Pong, W.W., Emnett, R.J., White, C.R., Gianino, S.M., Rodriguez, F.J. and Gutmann, D.H. (2011) Neurofibromatosis-1 heterozygosity increases microglia in a spatially and temporally restricted pattern relevant to mouse optic glioma formation and growth. *J. Neuropathol. Exp. Neurol.*, **70**, 51–62.
33. Daginakatte, G.C., Gianino, S.M., Zhao, N.W., Parsadanian, A.S. and Gutmann, D.H. (2008) Increased c-Jun-NH2-kinase signaling in neurofibromatosis-1 heterozygous microglia drives microglia activation and promotes optic glioma proliferation. *Cancer Res.*, **68**, 10358–10366.
34. Solga, A.C., Pong, W.W., Kim, K.Y., Cimino, P.J., Toonen, J.A., Walker, J., Wylie, T., Magrini, V., Griffith, M., Griffith, O.L. et al. (2015) RNA sequencing of tumor-associated microglia reveals Ccl5 as a stromal chemokine critical for neurofibromatosis-1 glioma growth. *Neoplasia*, **17**, 776–788.
35. Huang, C.Y., Fong, Y.C., Lee, C.Y., Chen, M.Y., Tsai, H.C., Hsu, H.C. and Tang, C.H. (2009) CCL5 increases lung cancer migration via PI3K, Akt and NF-kappaB pathways. *Biochem. Pharmacol.*, **77**, 794–803.
36. Tyner, J.W., Uchida, O., Kajiwar, N., Kim, E.Y., Patel, A.C., O'Sullivan, M.P., Walter, M.J., Schwendener, R.A., Cook, D.N., Danoff, T.M. et al. (2005) CCL5-CCR5 interaction provides anti-apoptotic signals for macrophage survival during viral infection. *Nat. Med.*, **11**, 1180–1187.
37. Liu, G.T., Chen, H.T., Tsou, H.K., Tan, T.W., Fong, Y.C., Chen, P.C., Yang, W.H., Wang, S.W., Chen, J.C. and Tang, C.H. (2014) CCL5 promotes VEGF-dependent angiogenesis by down-regulating miR-200b through PI3K/Akt signaling pathway in human chondrosarcoma cells. *Oncotarget*, **5**, 10718–10731.
38. Vincent, E.E., Elder, D.J., Thomas, E.C., Phillips, L., Morgan, C., Pawade, J., Sohail, M., May, M.T., Hetzel, M.R. and Tavare, J.M. (2011) Akt phosphorylation on Thr308 but not on Ser473 correlates with Akt protein kinase activity in human non-small cell lung cancer. *Br. J. Cancer*, **104**, 1755–1761.
39. Messiaen, L., Yao, S., Brems, H., Callens, T., Sathienkijkanchai, A., Denayer, E., Spencer, E., Arn, P., Babovic-Vuksanovic, D., Bay, C. et al. (2009) Clinical and mutational spectrum of neurofibromatosis type 1-like syndrome. *JAMA*, **302**, 2111–2118.
40. Sabbagh, A., Pasmant, E., Laurendeau, I., Parfait, B., Barbarot, S., Guillot, B., Combemale, P., Ferkal, S., Vidaud, M., Aubourg, P. et al. (2009) Unravelling the genetic basis of variable clinical expression in neurofibromatosis 1. *Hum. Mol. Genet.*, **18**, 2768–2778.
41. Rojnuangnit, K., Xie, J., Gomes, A., Sharp, A., Callens, T., Chen, Y., Liu, Y., Cochran, M., Abbott, M.A., Atkin, J. et al. (2015) High incidence of Noonan syndrome features including short stature and pulmonic stenosis in patients carrying NF1 missense mutations affecting p.Arg1809: genotype-phenotype correlation. *Hum. Mutat.*, **36**, 1052–1063.
42. Alkindy, A., Chuzhanova, N., Kini, U., Cooper, D.N. and Upadhyaya, M. (2012) Genotype-phenotype associations in neurofibromatosis type 1 (NF1): an increased risk of tumor complications in patients with NF1 splice-site mutations? *Hum. Genomics*, **6**, 12.
43. Gelfman, C.M., Vogel, P., Issa, T.M., Turner, C.A., Lee, W.S., Kornfeld, S. and Rice, D.S. (2007) Mice lacking alpha/beta subunits of GlcNAc-1-phosphotransferase exhibit growth retardation, retinal degeneration, and secretory cell lesions. *Invest. Ophthalmol. Vis. Sci.*, **48**, 5221–5228.
44. Paton, L., Bitoun, E., Kenyon, J., Priestman, D.A., Oliver, P.L., Edwards, B., Platt, F.M. and Davies, K.E. (2014) A novel mouse model of a patient mucopolidosis II mutation recapitulates disease pathology. *J. Biol. Chem.*, **289**, 26709–26721.
45. Dalin, M.G., Zou, Z., Scharin-Tang, M., Safari, R., Karlsson, C. and Bergh, M.O. (2014) Myocardial KRAS(G12D) expression does not cause cardiomyopathy in mice. *Cardiovasc. Res.*, **101**, 229–235.
46. Hernandez-Porras, I., Fabbiano, S., Schuhmacher, A.J., Aicher, A., Canamero, M., Camara, J.A., Cusso, L., Desco, M., Heeschen, C., Mulero, F. et al. (2014) K-RasV14I recapitulates Noonan syndrome in mice. *Proc. Natl. Acad. Sci. USA*, **111**, 16395–16400.
47. Dasgupta, B., Yi, Y., Chen, D.Y., Weber, J.D. and Gutmann, D.H. (2005) Proteomic analysis reveals hyperactivation of the mammalian target of rapamycin pathway in neurofibromatosis 1-associated human and mouse brain tumors. *Cancer Res.*, **65**, 2755–2760.
48. Lee, D.Y., Yeh, T.H., Emnett, R.J., White, C.R. and Gutmann, D.H. (2010) Neurofibromatosis-1 regulates neuroglial progenitor proliferation and glial differentiation in a brain region-specific manner. *Genes Dev.*, **24**, 2317–2329.
49. Dasgupta, B., Li, W., Perry, A. and Gutmann, D.H. (2005) Glioma formation in neurofibromatosis 1 reflects preferential activation of K-RAS in astrocytes. *Cancer Res.*, **65**, 236–245.
50. Roth, J.J., Santi, M., Rorke-Adams, L.B., Harding, B.N., Busse, T.M., Tooke, L.S. and Biegel, J.A. (2014) Diagnostic application of high resolution single nucleotide polymorphism array analysis for children with brain tumors. *Cancer Genet.*, **207**, 111–123.
51. Diggs-Andrews, K.A., Brown, J.A., Gianino, S.M., Rubin, J.B., Wozniak, D.F. and Gutmann, D.H. (2014) Sex is a major

- determinant of neuronal dysfunction in neurofibromatosis type 1. *Ann. Neurol.*, **75**, 309–316.
52. Warrington, N.M., Sun, T., Luo, J., McKinstry, R.C., Parkin, P.C., Ganzhorn, S., Spoljaric, D., Albers, A.C., Merkelson, A., Stewart, D.R. et al. (2015) The cyclic AMP pathway is a sex-specific modifier of glioma risk in type I neurofibromatosis patients. *Cancer Res.*, **75**, 16–21.
 53. Kaul, A., Toonen, J.A., Gianino, S.M. and Gutmann, D.H. (2015) The impact of coexisting genetic mutations on murine optic glioma biology. *Neuro. Oncol.*, **17**, 670–677.
 54. Brown, J.A., Gianino, S.M. and Gutmann, D.H. (2010) Defective cAMP generation underlies the sensitivity of CNS neurons to neurofibromatosis-1 heterozygosity. *J. Neurosci.*, **30**, 5579–5589.